Graphene functionalized with partially deacetylated chitin extracted from shrimp shell waste

B. Guerrero-Rodríguez [a], A. Jamett [a], L. Layana [a], C. Berrezueta-Palacios [a, b], S. Cortez-Gómez [a], S. Briceño [a]*, J. Lobos [a]*

[a] Yachay Tech University, School of Physical Sciences and Nanotechnology, 100119-Urcuquí, Ecuador.
[b] Department of Physics, Freie Universität Berlin, Berlin 14195, Germany.

*Corresponding authors, E-mail: sbricenio@yachaytech.edu.ec and jlobos@yachaytech.edu.ec

Received: 18-05-2021 Accepted: 06-08-2021
Published: 17-09-2021

ABSTRACT
The understanding of the interaction between graphene with chitinous polymers remains a challenge. Herein, we propose the extraction of partially deacetylated chitin from *Litopeneaus Vannamei* shrimp's waste (C_H30) to produce a nanocomposite film with graphene and compared it with a high deacetylated chitosan (C_H75). Structural characterization was carried out by X-ray Photoelectron Spectroscopy (XPS), Fourier Transform Infrared Spectroscopy (FTIR), Raman, Scanning Electron Microscopy (SEM), and Thermogravimetric Analysis (TGA-DTG). Our findings reveal the successful functionalization of graphene with chitin to form a nanocomposite film. These findings shed light on the interaction between graphene and chitinous polymers in regards to give an additional value to shrimp shell waste.

Keywords: Chitin, chitosan, graphene, nanocomposite, nanoparticles.

Grafeno funcionalizado con quitina parcialmente desacetilada extraída de desechos de cáscaras de camarón

RESUMEN
La compresión de la interacción del grafeno con polímeros quitinosos es todavía un desafío. En este trabajo, se propone la extracción de quitina parcialmente desacetilada a partir de residuos de cascara de camarón *Litopeneaus Vannamei* (C_H30), comparado con quitosano altamente desacetilado (C_H75) para formar un nanocomposito con grafeno. La caracterización estructural se llevó a cabo usando Espectroscopía Fotoelectrónica de Rayos-X (XPS), Espectroscopia de Infrarrojo por Transformada de Fourier (FTIR), Espectroscopía Raman, Microscopía Electrónica de Barrido (SEM), y Análisis Termogravimétrico (TGA-DTG). Los resultados revelan la funcionalización exitosa del grafeno con quitina para formar el nanocomposito. Estos resultados dan luz en la interacción entre el grafeno y polímeros quitinosos en lo que se refiere a dar un valor agregado a los residuos de cáscara de camarón.

Palabras claves: Quitina, quitosano, grafeno, nanocomposito, nanopartículas.

INTRODUCTION

N-acetyl-D-glucosamine is among the most abundant biopolymers on Earth. The majority of its extraction derives from crustacean shell waste. By convention, N-acetyl-D-glucosamine is identified as chitin when the N-deacetylation degree (DD) is below 50% and as chitosan when the DD is larger than 50% [1, 2]. Chitin and chitosan are both biocompatible, biodegradable and nontoxic polymers, which can be easily processed into films, fibbers, membranes, and scaffolds [3]. It has been reported [4] that the inherent properties of biopolymers cab be enhanced by the implementation of different nanofillers, mainly as carbon allotropes where the biopolymer serves as the hosting material for the resulting nanocomposite.

Chitosan/chitin nanocomposites made with Graphene derivatives such as reduced graphene oxide and graphene oxide have come into attention due to the novel properties that graphene exhibit. So far, there are reports [5] in biotechnology related to these materials, e.g. aerogel beads for bilirubin adsorption bio-anodes with enhanced electrochemical properties [6], fabrication of screws with steel concrete structure that show high bending strength [7], and nanocomposites membranes with chitosan for the wastewater treatment [8]. Even though graphene shows properties when compared with other graphene derivatives,

an experimental work related to pristine graphene with *Litopeneaus Vannamei* chitin composite has not been studied yet.

Computational modelling suggests a graphene chitosan membrane have a significant tensile module in comparison with oxidized graphene [9]. Prompt by these results, in this work we present an extraction process of partially deacetylated chitin from *Litopeneaus Vannamei* shrimp's waste (C_H30) to produce a nanocomposite film with graphene and compared it with a high deacetylated chitosan (C_H75). As the physicochemical properties of chitin vs chitosan, such as solubility, hydrophobicity and crystallinity, change upon the number of acetyl groups in the glucosamine chain, it is expected that the functionalization with graphene show different features.

MATERIALS AND METHODS

Partially deacetylated chitin (C_H30) extracted from *Litopeneaus Vannamei* shells from Manabí-Ecuador (30% deacetylated). Chitosan (C_H75) from Sigma Aldrich (75-85% deacetylated) with 50,000-190,000 Da (based on viscosity). Reagent-grade products employed are hydrochloric acid (37%), sodium hydroxide pellets, and acetic acid (99%), from Fisher Scientific. Few-layer graphene platelets, from Elicarb® Premium Grade SP8073P.

Extraction of partially deacetylated chitin (C_H30).

Chitin/chitosan synthesis process consists in three main steps: deproteinization, demineralization and deacetylation. *Litopeneaus Vannamei* shrimp shells waste were obtained from Manabí-Ecuador, washed with distilled water, dried at 80°C for 12 h, and pulverized with an industrial blender. A batch of 100 g of powder was deproteinized with 1080 mL of NaOH (4%, m/v) at 80°C for 3 h, then vacuum filtered and washed with distilled water. The demineralization process was performed with an acid treatment using 500 mL of hydrochloric acid (1 M) for 18 h in order to dissolve the calcium carbonate present in the powder, next the sample was vacuum filtered and washed with distilled water. The deacetylation process was carried by treating the sample with 800 mL of NaOH (50% v/v) in constant magnetic stirring for 1 h at 100°C, later the sample was vacuum filtered, washed with distilled water, and dried at 65°C [10]. That dried powder is partially-deacetylated chitin (C_H30) (see figure 1). Herein, we extracted a partially deacetylated chitin from *Litopeneaus Vannamei* shrimp shell waste with a 30% DD and compared to purchased chitosan with 75% DD to form a nanocomposite films with graphene.

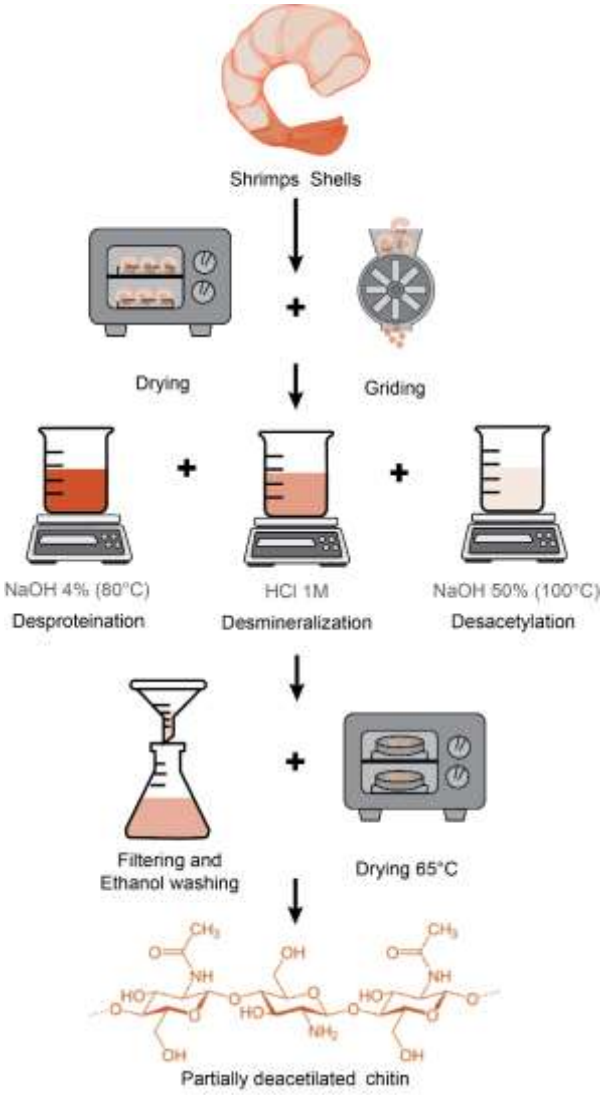

Fig. 1. Extraction process of partially deacetylated chitin (C_H30).

Synthesis of deacetylated chitin-graphene (G_RC_H30) and chitosan-graphene (G_RC_H75) nanocomposite films.

0.1 g of C_H30 powder was dissolved in 10 mL of acetic acid (2%) at 80°C with constant magnetic stirring for 15 min., simultaneously, 0.1 g of graphene platelets was sonicated in 10 mL of acetic acid (2%) for 1 h. Then both samples were mixed, 9 mL of C_H30 in acetic acid was mixed with 1 mL of graphene, to prepare the nanocomposite solution. The nanocomposite solution was sonicated for 1.5 h, and then dried at 60°C for 12 h to obtain the G_RC_H30 nanocomposite film. Afterwards, sample G_RC_H75 was prepared following the same procedure described but using chitosan powder (C_H75).

Characterization.

Chemical composition was measured by X-ray Photoelectron Spectroscopy (XPS), VERSAPROBE PHI5000 from Physical Electronics, equipped with a Monochromatic Al Kα X-Ray with energy resolution 0.5 eV. For the compensation of built-up charge on the sample's surface during measurements, a dual-beam neutralization charge composed of an electron gun (∼1 eV) and the Argon Ion gun (≤ 10 eV) was used. All binding energies were calibrated to the C1s peak at 284.8 eV. Fourier Transform Infrared Spectroscopy (FTIR) was performed using a PerkinElmer 1650 spectrometer between 4000 and 500 cm^{-1}. Scanning Electron micrographs were acquired by a FEI Inspect F50 with an acceleration of 8-10 KeV. Raman measurements were acquired using a HORIBA LabRAM HR Evolution spectrometer at 532 nm. Thermogravimetric Analysis (TGA) was measured using a TGA-Q 500, TA Instruments, DE, in a nitrogen atmosphere from 20°C to 600°C at 15°C/min.

RESULTS AND DISCUSSION

X-Ray Photoelectron Spectroscopy (XPS).

The elemental composition and analysis of samples C_H30 and C_H75 was identified by XPS. Both samples show the expected elements of chitin/chitosan in the XPS survey spectrum (C, O and N). In addition, traces of Ca were found which is be attributed to the residue of the source material (shrimp exoskeleton) [11, 12].

Figure 2 shows the recorded of the three main peaks present corresponding to C1s, N1s, and O1s core-level spectra from samples C_H30 and C_H75. These spectra are calibrated with respect to the first component (C1) of the C1s peak located at 284.8 eV [13]. The C1s core level of chitin C_H30 sample is decomposed into three components c1 at 284.8 eV, c2 at 286,3 eV and c3 at 287.9 eV (see figure 2a). which are assigned to C-C bonding or adventitious carbon present in aliphatic groups, to C–N, C=N, C–O or C–O–C groups and the C=O or O–C–O bonding respectively [11]. For chitosan sample C_H75, also three intensity peaks are observed in the range of 287-284 eV (figure 2b). The N1s region of the XPS spectra of C_H30 and C_H75 are shown in figure 2c and 2d. These spectra can be reproduced using two components: a high-intensity component corresponding to the unprotonated amine (N1) and a low-intensity component (N2) at a higher binding energy corresponding to the protonated amine [11, 14]. Even though a nitrogen chemical environment is expected for chitin and chitosan, N2 component arises from the acetic acid's dissolution process which induces protonation of the amine segments. Some of these amine groups will remain protonated after drying the chitin/chitosan [15]. The O1s spectra contains three peaks assigned to oxygen in carbonyl groups, similar to those found in polyacrylamide (O1 at 531 eV). The most intense component O2, attributed to –O– or glycosides group (533.3 eV). O3 is assigned to -OH or hydroxyl groups (figure 2e and 2f), which are in accordance with the ranges found for cellulose [16]. The chitin C_H30 sample shows 73.39% C, 5.17% N, 21.01% O, and 0.43% Ca, while the chitosan C_H75 shows 67.00% C, 6.58% N, 25.79% O and 0.63% Ca. These results are presented in table 1. The theoretical atomic composition of a 70% deacetylated chitosan is 55.00% C, 9.00% N, and 36.00% O, according to Matienzo Winnacker [11]. The difference in the atomic percentage of samples

C_H30 and C_H75 with theoretical chitosan relies on the different deacetylation degree. This correlation between a lower carbon content with a higher degree of deacetylation has also been reported by [17], which can be correlated with the relative amount of carbon atoms contributing to the component C3 of the C1s spectrum in the C_H30 (15.5%) with respect to C_H75 (8.17 %) that suggest a higher concentration of C=O or O–C–O bonding. Additionally, the amount of oxygen atoms contributing to the component O1 corresponding to carbonyl groups is higher in C_H30 (11.13 %) than in C_H75 (8.68 %). These groups are present in the acetyl group, expected to be removed from the chitosan in the process of deacetylation. A higher amount of these groups would suggest a lower degree of deacetylation, confirming a lower degree of deacetylation in the C_H30 sample.

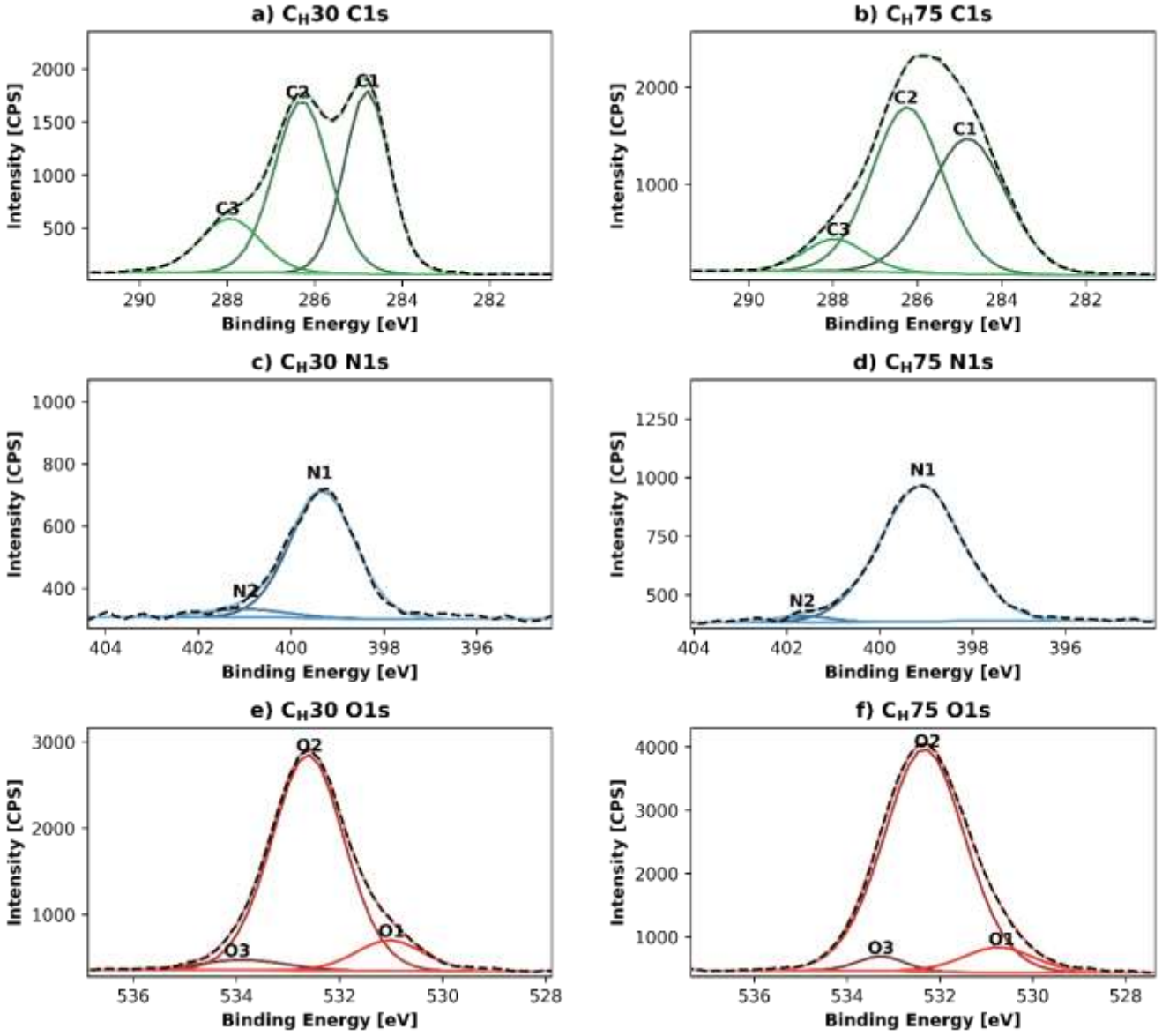

Fig. 2. High resolution XPS of partially deacetylated chitin (C_H30), and chitosan (C_H75) a), b) C1s; c), d) N1s; and e), f) O1s respectively.

Table 1. Elemental composition and deconvolution of C1s, N1s and O1s photoelectron for C_H30 and C_H75 samples.

ELEMENT		C_H30		C_H75		ASSIGNMENTS
		BE [eV]	AC [%]	BE [eV]	AC [%]	
C1s	C1	284.8	39.35	284.8	42.97	C–C or adventitious carbon
	C2	286.3	45.15	286.2	48.85	C–N, C=N, C–O or C–O–C
	C3	287.9	15.5	288.0	8.17	C=O or O–C–O
	Total C	-	73.39	-	67	-
N1s	N1	399.3	92.55	399.1	97.18	non-protonated amine
	N2	401.0	7.45	401.6	2.18	protonated amine
	Total N	-	5.17	-	6.58	-
O1s	O1	531.0	11.13	530.7	8.68	carbonyl groups
	O2	532.6	84.08	532.3	87.96	–O– groups
	O3	533.9	4.79	533.3	3.36	–OH groups
	Total O	-	21.01	-	25.79	-
Ca	Total Ca	-	0.43	-	0.63	-

Raman spectroscopy.

Raman spectroscopy confirms the presence of graphene and not graphene derivatives. The D, G and 2D lines of graphene pristine are at around 1342 cm^{-1}, 1572 cm^{-1} and 2695 cm^{-1} respectively as shown in figure 3.

An interesting feature of the Raman spectra is the notorious upshift of the D, G and 2D lines in the spectrum of G_RC_H30. It has been previously reported [18, 19] that the 2D line upshifts as the number of graphene layers' increase, and also the line shape changes. In the spectrum of G_RC_H30, the upshift of 23 cm^{-1} of the 2D line might suggest that there is either an agglomeration or more stacking of graphene layers, along with the partially deacetylated chitin chains into the system of the G_RC_H30. Also, the ratio between the intensity (I) of the G and 2D line gives information about the number of graphene layers. In this case, the ratio IG/I2D of the nanocomposite film (2.66 for G_RC_H30 and 2.75 for and G_RC_H75) has increased in comparison with the ratio of the pristine sample (3.46), perhaps indicating a successful intercalation of partially deacetylated chitin and chitosan in graphene [20].

Ferrari *et al*. also pointed out that an upshift in the G line is due to the chemical doping [18], which suggest an interaction of partially deacetylated chitin and chitosan with graphene. This chemical doping is described in figure 4 with FTIR.

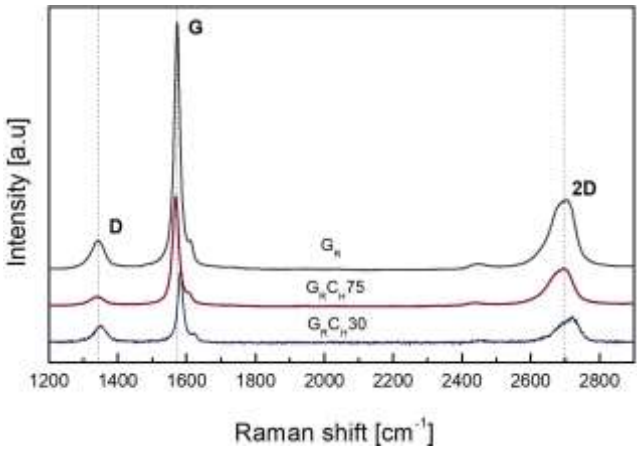

Fig. 3. Raman spectrum of graphene, chitosan-graphene nanocomposite film (G_RC_H75) and partially deacetylated chitin-graphene nanocomposite film, with an excitation laser of 532 nm.

Fourier Transform Infrared Spectroscopy (FTIR).

Figure 4 shows the characteristics peaks of graphene at 1632 cm^{-1} attributed to C=C vibrations, and related to the carbon sp2 orbitals [21, 22]. A weak signal at 1737 cm^{-1} is attributed to the stretching vibration of the C=O group and related to the band at 1240 cm^{-1}, demonstrating the formation of

carboxylic acid groups on the graphene surface [23, 24]. Partially deacetylated chitin and chitosan FTIR spectra exhibit a broad peak at 3450 cm^{-1} corresponding to the O-H vibration, which is overlapping with the N-H groups stretching [25], while the absorption corresponds to the C-H stretch at 2870 cm^{-1} [26]. The peaks at 1624 cm^{-1} and 1650 cm^{-1} are attributed to the carbonyl stretching (C=O) of amide I for chitin [27], when for chitosan the peak of amide I is at 1650 cm^{-1} [26]. For sample C_H30 it is observed that both peaks for amide I are clearly differentiated and do not overlap each other, meanwhile with C_H75 it presents a single peak. This characteristic of C_H30 is due to the higher number of acetyl groups compared to C_H75. The band at 1560 cm^{-1} corresponds to the N-H bending of the amide II [27]. The bands of the amide I also indicate the grade of acetylation of the biopolymer [28].

The degree of deacetylation was calculated using the bands at 3450 cm^{-1} and 1650 cm^{-1} [28], obtaining 79% DD for C_H75 and 35% DD for C_H30. The spectra of G_RC_H75 and G_RC_H30 nanocomposite differ from the spectra of C_H30 and C_H75, demonstrating that the biopolymers interact with the graphene.

The bands at 1650 cm^{-1} and 1624 cm^{-1} disappear, indicating that the amide I group's hydrogen atoms are interacting with the carbon atoms of the graphene layer [29]. The band at 3450 cm^{-1} of both chitinous polymers became narrower, confirming an interaction of the OH groups with the carbon atoms on the layer of graphene [29, 30].

The reduction of the amide II band (1560 cm^{-1}) in the nanocomposite also confirms the interaction between the hydrogen with the graphene [27].

G_RC_H30 presents a wider peak at 1540 cm^{-1} than G_RC_H75, meaning that partially deacetylated chitin nanocomposite interacts with a higher amount of graphene in comparison to the chitosan nanocomposite. It can be observed that there exists a peak around 2870 cm^{-1} and 2920 cm^{-1} in the partially deacetylated chitin nanocomposite that is not present in the chitosan nanocomposite, due to the C-H stretch.

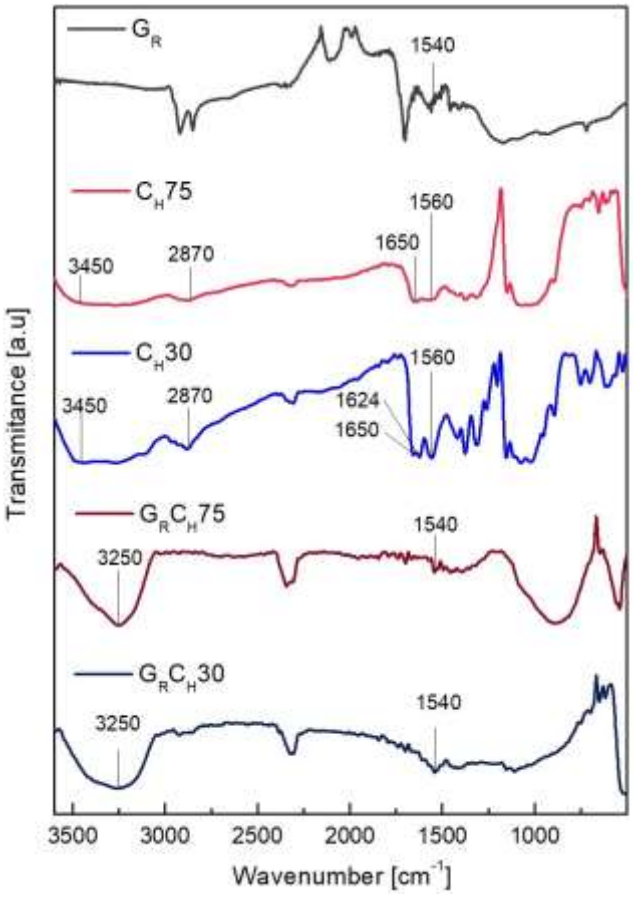

Fig. 4. FTIR of graphene G_R, chitosan (C_H75), partially decetylated chitin (C_H30), chitosan-graphene nanocomposite (G_RC_H75) and partially deacetylated chitin-graphene nanocomposite (G_RC_H30).

Scanning Electron Microscopy (SEM).

Figure 5 shows the Scanning Electron micrograph of (a) partially deacetylated chitin (C_H30), (b) chitosan C_H75, (c) partially deacetylated chitin - graphene nanocomposite (G_RC_H30), and (d) chitosan-graphene nanocomposite (G_RC_H75).

Figures 5a and 5b, show the presence of agglomerations of semispherical nanoparticles of partially deacetylated chitin and chitosan with an average particle size of 30 ± 10 nm, and 60 ± 20 nm respectively. These nanoparticles are formed in consequence of the hydrolysis caused by the acidic media and the ultrasonication treatment during the synthesis of the nanocomposite [31]. Figures 5c and 5d show the formation

of the nanocomposite by the incorporation of the chitinous polymer on graphene.

In these figures, it is observed that graphene has an average flake size of 1.6 ± 0.5 µm and undergoes severe agglomeration, due to the graphene is a highly conjugated structure, in which the unpaired electrons of carbon atoms form p bonds throughout the layer, leading to the overlapping of graphene sheets due to van der Waals forces and electrostatic interactions [29]. Nevertheless, in figure 5c the graphene is homogeneously dispersed compared to figure 5d, this is related to the effect of the lowest degree of deacetylation [20] and the intercalation of partially deacetylated chitin in graphene as we reported in figures 3 and 4 respectively.

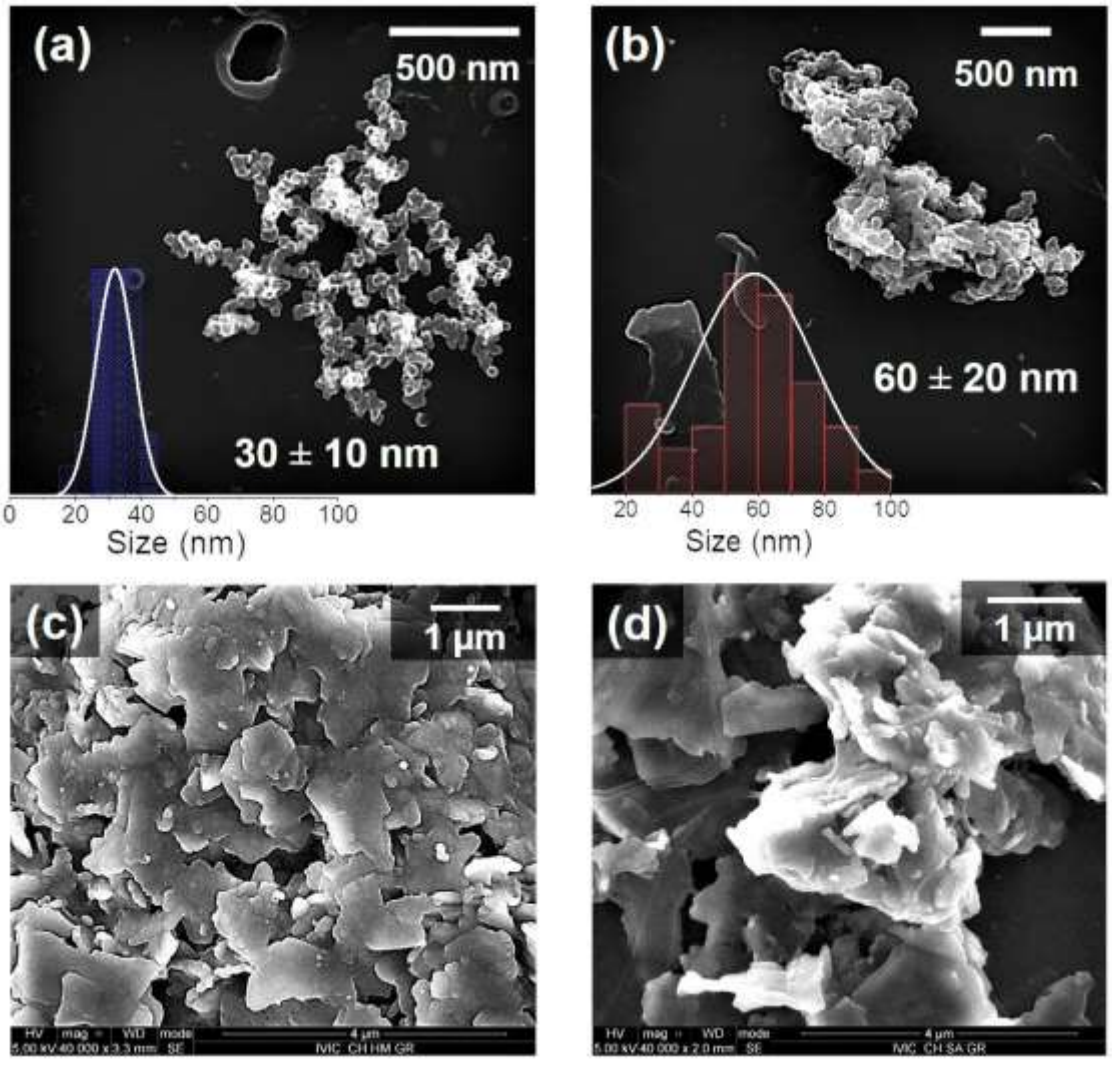

Fig. 5. SEM micrographs of a) partially deacetylated chitin (C_H30), b) chitosan C_H75, c) partially deacetylated chitin - graphene nanocomposite (G_RC_H30) and d) chitosan-graphene nanocomposite (G_RC_H75).

Thermogravimetric Analysis (TGA-DTG).

Thermogravimetric measurements in nitrogen-atmosphere indicate that the partially deacetylated chitin and chitosan samples decompose in two steps (see figure 6a and 6b; table 2). The first one indicates that both samples contain about 8% to 10% of adsorbed water, evaporated at a low temperature; this means that the water is physically adsorbed to partially deacetylated chitin and chitosan molecules [30]. The second one is the actual decomposition process, caused by the rupture of the polysaccharide chains via dehydration and deamination [33]. The partially deacetylated chitin degradation started at 171°C and with a

mass loss of 53%; chitosan degradation started at 159°C with a 55% drop of mass. A high starting degradation temperature of chitinous polymers is attributed to the high thermal stability of the acetylated side-chains [33]; hence, partially deacetylated chitin has a higher thermal stability than chitosan (see table 2).

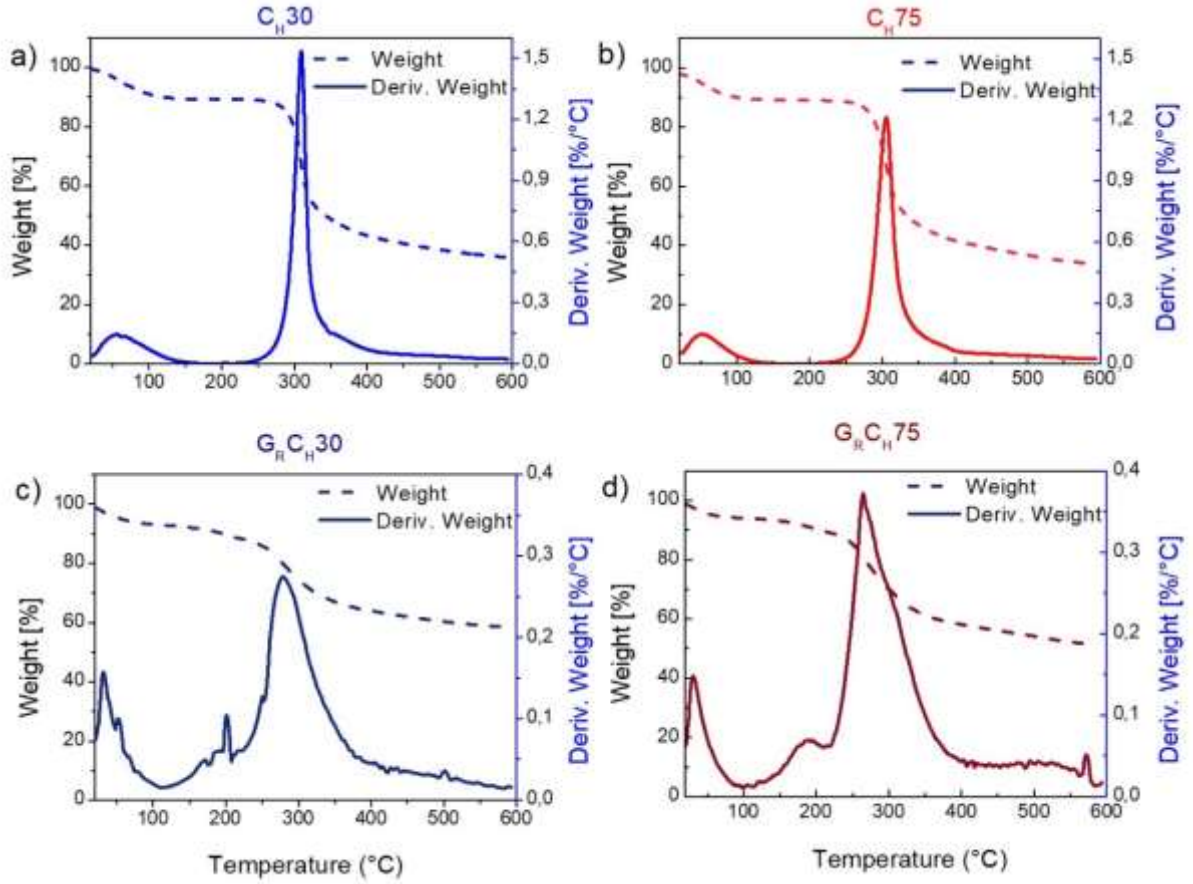

Fig. 6. TGA and DTG curves of a) partially deacetylated chitin (C_H30), b) chitosan (C_H75), c) partially deacetylatedchitin-graphene nanocomposite (G_RC_H30) and d) chitosan-graphene nanocomposite (G_RC_H75).

Table 2. Thermal parameters (degradation temperatures and weight loss) obtained from thermogravimetric analysis of partially deacetylated chitin, chitosan, and nanocomposite with graphene.

	Td1			Td2			Td3			Residue [%]
SAMPLE	Range [˚C]	Peak [˚C]	Weight Loss [%]	Range [˚C]	Peak [˚C]	Weight Loss [%]	Range [˚C]	Peak [˚C]	Weight Loss [%]	At 600 ˚C
C_H30	20-171	56	10.08	-	-	-	171-594	309	53.55	35.84
C_H75	21-159	52	8.76	-	-	-	159-593	305	55.48	33.75
G_RC_H30	21-111	32	5.85	111-208	201	3.93	208-593	278	30.6	58.42
G_RC_H75	21-91	31	4.64	91-210	186	5.49	210-593	265	38.69	50.99
Chitosan Film*	20-105	45	10	105-234	168	11	234-600	274	43	36

TGA curves and the corresponding derivatograms (DTG) of partially deacetylated chitin-graphene and chitosan-graphene nanocomposites are shown in figure 6c and 6d. In DTG we identify three significant peaks for the G_RC_H30 and

G_RC_H75 nanocomposites. According to Zawadzki Kaczmarek [34] the first peak between 30 – 40°C is explained as the release of physisorbed water, while the second peak around 180°C is due to the evaporation of strongly hydrogen-bonded water. The third peak between 260 – 280°C is caused by chitosan chains' depolymerization and pyranose rings' decomposition [32, 33]. Chitosan's thermal degradation occurs via a free radical mechanism, the intermediate radical products form crosslinked structures [34]. After comparing the char residue in table 2, the difference between 50% for G_RC_H75 and 58% for G_RC_H30 mirrors the higher presence of graphene in G_RC_H30. The extraction of partially deacetylated chitin from shrimp shell waste was confirmed qualitatively by the high carbon content in XPS and the relation between 3450 cm^{-1} and 1650 cm^{-1} bands in FTIR analysis. The successful synthesis of a composite film with partially deacetylated chitin and graphene was corroborated by FTIR, Raman and SEM.

The differences in the TGA show the higher interaction with water in the composite samples, lowering the decomposition temperature of the polymers and widening the peak of the decomposition steps. The lower peak on the derivate weight of the G_RC_H30 indicates the possibility of agglomeration or extra stacking of graphene layers inside the partially deacetylated chitin matrix, as we indicated through Raman spectra analysis.

Furthermore, this graphene agglomeration is reflected in the SEM micrographs of the nanocomposites, showing that the graphene in G_RC_H30 is distinctly more homogeneously dispersed when compared to G_RC_H75, due to the greater amount of acetyl groups and the interaction between the amides and OH groups with the surface of the graphene, (see figure 7).

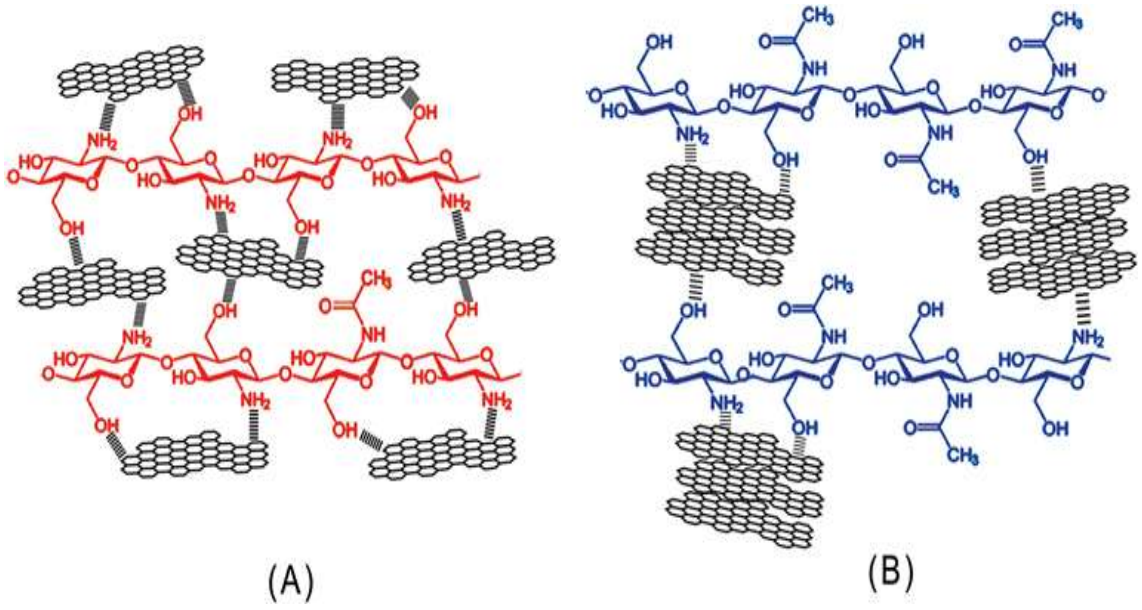

Fig.7. Interaction scheme of (A) chitosan-graphene nanocomposite (G_RC_H75) and (B) partially deacetylated chitin-graphene nanocomposite (G_RC_H30).

CONCLUSIONS

Partially deacetylated chitin was successfully extracted from shrimp shell waste with a DD of 30% as confirmed by FTIR. XPS also supports that the content of acetyl groups in C_H30 is higher than the 75% DD purchased chitosan (C_H75). C_H30 with a DD of 30% and chitosan biopolymers are used to obtain graphene nanocomposites films by a simple, low cost, and green-pathway. SEM micrographs showed the formation of nanoparticles of 30 nm of partially deacetylated chitin and 60 nm of chitosan, caused by the chemical and physical treatment during the experimental setup and the formation of the nanocomposite.

Finally, we have achieved an experimental setup for the functionalization of graphene with partially deacetylated chitin to obtain a nanocomposite film as a potential add value to the shrimp shell waste.

ACKNOWLEDGEMENT

The authors thanks to Victor Vicente Vilas for the support in the chitin extraction process. Thanks to Lisbeth Lozada and Joseba Echebarrieta in the Instituto Venezolano de Investigaciones Científicas (IVIC) for their support in sample preparation and SEM observation. Also, thanks to Dr. Carla Bittencourt and the University of Mons for performing the XPS measurements of the samples. Finally, thanks to Eng. Salomé Galeas, Eng. Orlando Campaña and Dr. Víctor Guerrero from Escuela Politécnica Nacional for the thermogravimetric characterization and Veronica Lobos for the grammar English revision.

REFERENCES

[1] Sashiwa H., Harding D. (2018) "Advances in Marine Chitin and Chitosan II, 2017" *MDPI* AG-Multidisciplinary Digital Publishing Institute.

[2] Yanat M., Schroën K. (2021) "Preparation methods and applications of chitosan nanoparticles; with an outlook toward reinforcement of biodegradable packaging" *React. Funct. Polym.* 161:104849.

[3] Rinaudo M. (2006) "Chitin and chitosan: Properties and applications" *Prog. Polym. Sci.* 31(7):603-632.

[4] Ahmed M.J., Hameed B.H., Hummadi E.H. (2020) "Review on recent progress in chitosan/chitin-carbonaceous material composites for the adsorption of water pollutants" *Carbohydr. Polym.* 247:116690.

[5] Song Z., Li G., Guan F., Liu W. (2018) "Application of chitin/chitosan and their derivatives in the papermaking industry" *Polymers* 10(4):389.

[6] Haque S. ul, Nasar A., Rahman M.M. (2020) "Applications of chitosan (CHI)-reduced graphene oxide (rGO)-polyaniline (PAni) conducting composite electrode for energy generation in glucose biofuel cell" *Sci. Rep.* 10(1):10428

[7] Jin X., Li G., Jiang H., Zhou Y., Zhang W., Bao X., Wang Z., Hu, Q. (2019) "High strength graphene oxide/chitosan composite screws with a steel-concrete structure" *Carbohydr. Polym.* 214:167-173

[8] Ou X., Yang X., Zheng J., Liu M. (2019) "Free-Standing Graphene Oxide–Chitin Nanocrystal Composite Membrane for Dye Adsorption and Oil/Water Separation" *ACS Sustainable Chem. Eng.* 7(15):13379-13390.

[9] Ebrahimi S., Rafii-Tabar H. (2015) "Influence of hydrogen functionalization on mechanical properties of graphene and CNT reinforced in chitosan biological polymer: Multi-scale computational modelling" *Comput. Mater. Sci.* 101:189-193.

[10] Younes I., Rinaudo M. (2015) "Chitin and chitosan preparation from marine sources. Structure, properties and applications" *Mar. Drugs* 13(3):1133-1174.

[11] Matienzo L.J., Winnacker S.K. (2002) "Dry processes for surface modification of a biopolymer: chitosan" *Macromol. Mater. Eng.* 287(12):871-880.

[12] Vieira R.S., Oliveira M.L.M., Guibal E., Rodríguez-Castellón E., Beppu M.M. (2011) "Copper, mercury and chromium adsorption on natural and crosslinked chitosan films: an XPS investigation of mechanism" *Colloids Surf., A* 374(1-3):108-114.

[13] Maachou H., Genet M.J., Aliouche D., Dupont-Gillain C.C., Rouxhet P.G. (2013) "XPS analysis of chitosan–hydroxyapatite biomaterials: from elements to compounds" *Surf. Interface Anal.* 45(7):1088-1097.

[14] Desai K., Kit K., Li J., Davidson P.M., Zivanovic S., Meyer H. (2009) "Nanofibrous chitosan non-wovens for filtration applications" *Polymer* 50(15):3661-3669.

[15] Okuyama K., Noguchi K., Kanenari M., Egawa T., Osawa K., Ogawa K. (2000) "Structural diversity of chitosan and its complexes" *Carbohydr. Polym.* 41(3):237-247.

[16] Beamson G., Briggs D. (1992) "High resolution monochromated X-ray photoelectron spectroscopy of organic polymers: A comparison between solid state data for organic polymers and gas phase data for small molecules" *Mol. Phys.* 76(4):919-936.

[17] Franca R., Mbeh D.A., Samani T.D., Le Tien C., Mateescu M.A., Yahia L.H., Sacher E. (2013) "The effect of ethylene oxide sterilization on the surface chemistry and in vitro cytotoxicity of several kinds of chitosan" *J. Biomed. Mater. Res. Part B* 101(8):1444-1455.

[18] Ferrari A.C., Meyer J.C., Scardaci V., Casiraghi C., Lazzeri M., Mauri F., Piscanec S., Jiang D., Novoselov K.S., Roth S., Geim A.K. (2006) "Raman spectrum of graphene and graphene layers" *Phys. Rev. Lett.* 97(18):187401.

[19] Silva D.L., Campos J.L.E., Fernandes T.F.D, Rocha J.N., Machado L.R.P, Soares E.M., Miquita D.R., Miranda H., Rabelo C., Vilela Neto O.P., Jorio A., Cançado L.G. (2020) "Raman spectroscopy analysis of number of layers in mass-produced graphene flakes" *Carbon* 161:181-189.

[20] Wang K., Ma Q., Pang K., Ding B., Zhang J., Duan Y. (2018) "One-pot synthesis of graphene/chitin nanofibers hybrids and their remarkable reinforcement on Poly(vinyl alcohol)" *Carbohydr. Polym.* 194:146-153.

[21] Buang N.A., Fadil F., Majid Z.A., Shahir S. (2012) "Characteristic of mild acid functionalized multiwalled carbon nanotubes towards high dispersion with low structural defects" *Digest Journal of Nanomaterials and Biostructures* 7(1):33-39.

[22] Kuila T., Bose S., Mishra A.K., Khanra P., Kim N.H., Lee J.H. (2012) "Effect of functionalized graphene on the physical properties of linear low density polyethylene nanocomposites" *Polym. Test.* 31(1):31-38.

[23] Montesa I., Muñoz E., Benito A.M., Maser W.K., Martinez M.T. (2007) "FTIR and Thermogravimetric Analysis of Biotin-Functionalized Single-Walled Carbon Nanotubes" *J. Nanosci. Nanotechnol.* 7(10):3473-3476.

[24] Yuen S-M., Ma C.M., Lin Y-Y., Kuan H-Ch. (2007) "Preparation, morphology and properties of acid and amine modified multiwalled carbon nanotube/polyimide composite" *Compos. Sci. Technol.* 67(11-12):2564-2573.

[25] Hajji S., Younes I., Ghorbel-Bellaaj O., Hajji R., Rinaudo M., Nasri M., Jellouli K. (2014) "Structural differences between chitin and chitosan extracted from three different marine sources" *Int. J. Biol. Macromol.* 65:298-306.

[26] Dassanayake R.S., Acharya S., Abidi N. (2018) "*Biopolymer-based materials from polysaccharides: Properties, processing, characterization and sorption applications*", Advanced Sorption Process Applications.

[27] Duarte M.L., Ferreira M.C., Marvao M.R., Rocha J. (2002) "An optimised method to determine the degree of acetylation of chitin and chitosan by FTIR spectroscopy" *Int. J. Biol. Macromol.* 31(1-3):1-8.

[28] Kasaai M.R. (2008) "A review of several reported procedures to determine the degree of N-acetylation for chitin and chitosan using infrared spectroscopy" *Carbohydr. Polym.* 71(4):497-508.

[29] Zhang H.P., Luo X.G., Lin X.Y., Lu X., Tang Y. (2016) "The molecular understanding of interfacial interactions of functionalized graphene and chitosan" *Appl. Surf. Sci.* 360:715-721.

[30] Shariatinia Z., Mazloom-Jalali A. (2020) "Molecular dynamics simulations on chitosan/graphene nanocomposites as anticancer drug delivery using systems" *Chin. J. Phys.* 66:362-382.

[31] Salaberria A.M., Labidi J., Fernandes S.C.M. (2015) "Different routes to turn chitin into stunning nano-objects" *Eur. Polym. J.* 68:503-515.

[32] Ziegler-Borowska M., Chełminiak D., Kaczmarek H. (2015) "Thermal stability of magnetic nanoparticles coated by blends of modified chitosan and

poly(quaternary ammonium) salt" *J. Therm. Anal. Calorim.* 119(1):499-506.

[33] Wanjun T., Cunxin W., Donghua C. (2005) "Kinetic studies on the pyrolysis of chitin and chitosan" *Polym. Degrad. Stab.* 87(3):389-394.

[34] Zawadzki J., Kaczmarek H. (2010) "Thermal treatment of chitosan in various conditions" *Carbohydr. Polym.* 80:394-400.